AAEC/E448

AAEC/E448

(2)

# AUSTRALIAN ATOMIC ENERGY COMMISSION

## RESEARCH ESTABLISHMENT

## LUCAS HEIGHTS

# AN APPARATUS FOR MEASURING THE ENERGY AND ANGULAR DISTRIBUTION OF ELECTRONS EJECTED IN ION-ATOM COLLISIONS

by

D.K. GIBSON
M.C.E. PETERSEN

July 1978

ISBN 0 642 59651 4

AUSTRALIAN ATOMIC ENERGY COMMISSION
RESEARCH ESTABLISHMENT
LUCAS HEIGHTS

# AN APPARATUS FOR MEASURING THE ENERGY AND ANGULAR DISTRIBUTION OF ELECTRONS EJECTED IN ION-ATOM COLLISIONS

by

D.K. GIBSON
M.C.E. PETERSEN

## ABSTRACT

There is a need for further data on the energy and angular distribution of electrons ejected from atoms and molecules by ion impact. An apparatus in which simultaneous measurements can be made of the energy and angular distributions of such electrons is described. The advantages of the apparatus are the possibility of fast data collection and the ability to make measurements over the whole range of scattering angle. Preliminary tests and a trial measurement with the apparatus are described.

National Library of Australia card number and ISBN 0 642 59651 4

The following descriptors have been selected from the INIS Thesaurus to describe the subject content of this report for information retrieval purposes. For further details please refer to IAEA-INIS-12 (INIS: Manual for Indexing) and IAEA-INIS-13 (INIS: Thesaurus) published in Vienna by the International Atomic Energy Agency.

ION-ATOM COLLISIONS; ANGULAR DISTRIBUTION; ELECTRONS; ENERGY SPECTRA; IONIZATION; LET; QUALITY FACTOR; DOSIMETRY; SECONDARY EMISSION DETECTORS

CONTENTS

## 1. INTRODUCTION

When energetic neutrons enter biological matter, the primary energy transfer events that occur are kinetic energy transfers to protons. This is because of the large quantities of hydrogen in the medium and the efficiency of energy transfer between particles of equal mass. As the resulting fast protons travel on through the matter, free electrons produced in ionising collisions move away from the particle track with a broad energy spectrum and at all angles to the track. From the point of view of radiation dosimetry, there are two reasons for wishing to obtain data on the angular and energy distributions of these ejected electrons. The first of these is concerned with improving knowledge of one of the present bases of radiation dosimetry, linear energy transfer (LET).

The earliest hypothesis in radiation dosimetry was that radiation damage to biological tissue, measured in terms of cell death or of induced changes that lead to cancer or genetic mutations, was proportional to the energy deposited per unit mass. As more knowledge was gained, it became clear that there are many departures from this rule, one of them being that densely ionising radiation causes greater damage for the same dose than weakly ionising radiation. This problem was dealt with in the practical sense by giving each type of radiation an empirical weighting factor, called the quality factor, relating its damaging power to that produced by 250 keV X-rays.

In an attempt to unify the concept of the quality factor, a correlation was made between the quality factors of different radiations and their linear energy transfers. The LET is the quantity of energy deposited per unit path length in the stopping medium by the radiation. There is an immediate difficulty in the concept of LET because of the unspecified cross section of the particle's track; this very much involves the role of the secondary electrons which serve to diffuse the deposition of energy.

$LET_{\Delta}$, a modified version of LET, has been introduced in which secondary electrons with energies in excess of $\Delta$ eV are excluded from the LET evaluation, as their energy is likely to be deposited so far from the centre of the track as not to be considered part of the track. As these concepts of LET are being used by the International Commission on Radiological Units and Measurements [ICRU 1970] to set quality factor values for radiations for which there is inadequate alternative information, the importance of refining the definition and understanding

of LET can be seen. With regard to the lack of understanding of the interrelationships between primary energy loss events, secondary molecular excitations and radical production and their overall biological signficance, it could be argued that the more correct $LET_{\Delta}$ should exclude secondary electrons of energy less than $\delta$ eV or, perhaps, exclude those of energy $< \delta$ eV and $> \Delta$ eV. A full knowledge of the energy and angular distribution of secondary electrons is clearly a prerequisite for the resolution of these uncertainties.

The second reason for our interest in the details of electron ejection is perhaps more basic. In a sense it negates the first as it is concerned with the search for an alternative to LET that will correlate with quality factor. There is evidence that LET is not an adequate criterion of radiation quality [Bewley 1968]. This is not unexpected as LET is essentially a macroscopic average quantity, whereas radiation damage, in which the effects are out of all proportion to the small quantities of energy absorbed, depends on the discrete nature of the processes involved. To achieve a better understanding of radiation dosimetry, there is clearly a need for much more data on the physical processes that can lead to modification of biochemical molecules. Because of the great complexity of biological systems, such information would have to be correlated with the results of biological experiments to obtain a better measure of radiation quality than LET.

These arguments show the importance of obtaining reliable data on angular and energy distributions of secondary electrons arising from proton bombardment of the atoms which constitute biological molecules or, better still, the molecules themselves. A review of measurements already made in this field has been published by Rudd [1975].
In summary, for angles between 10 and 160° and proton energies between 50 and 300 keV, measurements have been made in $H_2$, $N_2$, $O_2$, He, Ne and Ar by the group at Nebraska [Kuyatt & Jorgensen 1963; Rudd & Jorgensen 1963; Rudd *et al.* 1966; Crooks & Rudd 1971]. Other measurements have been made at higher energies, 300 to 1500 keV, between 20 and 130° in $H_2$ and $N_2$ [Toburen 1971; Toburen & Wilson 1972]. One measurement has been made at 0° in He with proton energy between 100 and 300 keV [Crooks & Rudd 1970]. A comprehensive tabulation of the available data for He has been published [Rudd *et al.* 1976]

The aim of the project described here is to extend the existing measurements in the following ways:

(i) Angular range : More emphasis would be given to small scattering angles and the zero deflection case.

(ii) Energy range : The incident ion energy range would be extended as low as possible to account for the entire stopping path of a 100 keV proton.

(iii) Target gases : $H_2$, $N_2$ and $O_2$ gases which are of biological interest, have been investigated but to date no carbon-containing molecules have been investigated; for example, deoxyribonucleic acid (DNA) has a chemical composition represented by $C_{10}\ H_{12.5}\ N_4\ O_6\ P$. Obviously $H_2O$ would also be a very relevant molecule.

## 2. APPARATUS

### 2.1 Design Considerations

There are various approaches to the problem of maintaining a pressure differential between the collision and the analysis-detection regions of an apparatus in which measurements are to be made over a wide angular range. In the apparatus used by Rudd and his co-workers, the analyser and detector were pumped and the pressure difference between this region and the collision region was maintained in a canal-like 'electron pipe'. On the other hand, with increasing frequency for wide-angle experiments, use is being made of arrays of capillary tubes to produce directed jets of target gases which provide high pressures over a small region. The advantage of such systems is that the two regions do not have to be separated from each other for differential pumping. Also, in the case of a secondary electron experiment, the electrons originate from a fairly small volume, *i.e.* the intersection of the proton beam and the gas jet.

The intention was to make this intersection the object focal point of an electrostatic energy analyser which led to an attempt to generalise the simplest electrostatic analyser in common use, the 45° parallel plate or Harrower analyser [Harrower 1955]. An analyser with two regions, as shown in Figure 1, was considered. The object and image points (O & I) are situated in a field-free region at distance x from the boundary of a plane electric field. A particle moves from O to I, entering and leaving the field region at angle $\Theta$. The distance between O and I can be expressed as

$$Y = x_o + 2\frac{x}{\tan\Theta}$$

which, using Harrower's expression for $x_o$, becomes

$$y = 2\frac{V}{E}\sin 2\Theta + 2\frac{x}{\tan\Theta} \quad , \qquad (1)$$

where E is the electric field strength and V is the energy of the particle in eV. As y is the distance between two focal points it is necessary that

$$\frac{dy}{d\Theta} = 4\frac{V}{E}\cos 2\Theta - 2\frac{x}{\sin^2\Theta} = 0 \quad .$$

This equation may be solved to give

$$\sin^2\Theta = \tfrac{1}{4}\left(1 \pm \sqrt{1 - \frac{4xE}{V}}\right) \quad .$$

As the aim is to maximise the distance x between the focal points and the field defining plates, let

$$\frac{4xE}{V} = 1 \quad , \qquad (2)$$

which leads to

$$\sin\Theta = \tfrac{1}{2} \text{ and } \Theta = 30° \quad . \qquad (3)$$

These values are suitable because x is finite and positive and, in fact, are especially advantageous because the second derivative is also zero, giving second order focusing. Putting the conditions (2) and (3) into the original equation for y, gives

$$\frac{y}{x} = 10.392.$$

Therefore a second order focusing analyser can be made using this geometric ratio and a 30° input angle.

The second order focusing properties can be demonstrated in the following way. Equation (1) may be written as

$$\frac{y}{x} = 2\cos\Theta\left(\frac{V}{4Ex}\,8\sin\Theta + \frac{1}{\sin\Theta}\right)$$

which, with the criterion in Equation (2), becomes

$$\frac{y}{x} = 2\cos\Theta\left(8\sin\Theta + \frac{1}{\sin\Theta}\right) \quad .$$

From this equation, the percentage deviation of $\frac{y}{x}$ from its value at $\Theta = 30°C$, given above, can be calculated. This deviation is plotted as a function of $\Theta$ in Figure 2. For comparison, the percentage deviation in $x_o$, the distance traversed by a particle in a 45° analyser (given by $x_o = 2\frac{V}{E}\sin 2\Theta$), is also shown. The figure illustrates the comparatively large angular range that can be accepted by the 30° analyser with

small changes in focal conditions. More general analyses of this type of analyser have been published [Harrower 1955; Green & Proca 1970].

As the aim was also to achieve angular analysis of the secondary electrons without moving the analyser, the 'fountain' configuration [Green & Proca 1970; Schmitz & Melhorn 1972] suggested itself. In this form, the object point radiates particles into an input annular slit. The electric field deflects them through a larger diameter annular output slit onto a circular image line. A proton beam can be fired through the object point and allowed to pass through the analyser *via* one point on the input slit and an exit hole in the back electrostatic plate (Figure 3). Because of the large disparity between the proton and electron energies, the energetic protons will pass through the field almost without deviation.

Electrons are generated at the object point by collisions between the beam and a jet of target gas atoms. A fraction of these electrons will pass through the analyser and be refocused at various points along the circular image line. Each point along this line corresponds to a certain angle between the trajectory of the ejected electron and the direction of the proton beam. By placing a number of small electron detectors around the image circle, electrons ejected at angles between 0 and 120°C can be counted simultaneously. By reversing the direction of the proton beam, measurements can be made for angles between 180 and 40°. The ability to cover the entire angular range is an advantage of this type of analyser. The detectable scattering angles between 0 and 120° are projected onto the analyser plane where they are spread through 180°. This is shown in Figure 4 where the relation between the scattering angle $\Theta$ and its projection, $\phi$, on the analyser plane is seen to be

$$\cos \phi = \frac{4 \cos \Theta - 1}{3} .$$

Measurements can be made of the relative energy and angular distributions only. Conversion to absolute double differential cross sections will require normalisation to previously established double differential cross sections. In the absence of suitable cross section data, the apparatus can be calibrated for a gas for which the ionisation cross section is known. The only difference in changing to a new target gas will be the viscosity of the flow through the jet, which can be measured fairly easily.

## 2.2 Construction

An apparatus has been constructed according to the principles discussed in Section 2.1. The basic dimensions are x = 15.4 mm and y = 160 mm, the outer diameter of the circular deflection plates being 400 mm. The spacing between the deflection plates is 30.8 mm, giving a nominal electron energy to analyser voltage ratio of 2. Four guard rings ensure a uniform field in the analyser region. The apparatus was constructed of stainless steel and annealed after manufacture to remove any ferromagnetic martensitic phase, induced by cold working, which could have led to anomalies in the magnetic field. The earthed plate (on the input and detector side) is made of three concentric sections. The inner circle is held in place by a 1 mm diameter stainless steel tube which serves to conduct the target gas to the jet. The outer annulus is attached to the central annulus by three or four stainless steel bars screwed to the two sections. These bars can be interchanged with the detector mounts so that they do not permanently interfere with any particular detector position. The slits formed by the space between the three elements of the input plate are sloped at angles displaced ± 4.5° from 30° to minimise the chance of scattering from the slits. The jet is made from a small piece of multichannel glass plate, the channels having a bore diameter of 5 μm. The diameter of the jet orifice is approximately 1 mm and its length is 3 mm.

The whole structure is mounted in a 450 mm diameter vacuum chamber on a 30° support, with sufficient adjustment to permit alignment of the required beam path with the actual beam. The proton beam is produced by a small 10–100 keV accelerator which was built for this purpose. The beam is admitted to the target chamber by a collimation tube. The collimation is effected by apertures of 1 mm and 0.3 mm separated by 200 mm. The final collimator (0.3 mm diameter) is biased at + 50 V, and is followed by a larger aperture (2 mm diameter) at earth potential to prevent the escape of electrons generated within the collimating tube.

Mullard B318 AL/01 channeltrons are used to detect the electrons. They are mounted in small shielded holders with suitable entry slits located at the analyser image points. The detectors can be readily moved from one angular position to another. At present three detectors are used, but the intention is to increase this number. In the preliminary experiments described in this report, the electron count rates have been recorded by means of an XY recorder driven by a ratemeter. In

normal operation, the counts from all the detectors will be recorded simultaneously by scalers in a Camac data acquisition system. The proton beam is monitored by a current-to-frequency converter driving a scaler.

## 3. CANCELLATION OF THE EARTH'S MAGNETIC FIELD

As is always the case in experiments with slow electrons, some account must be taken of the effect of the earth's magnetic field on the motion of the electrons. To see what value of magnetic field strength could be tolerated, some rough calculations have been made to estimate the effects of magnetic fields on the measurements. The problem can be split into two parts; the effect of fields normal to the analyser plates, affecting the angular measurements, and the effect of fields normal to the plane of the electron motion, affecting the energy measurement.

### (a) Angular measurement

A schematic diagram of the electron path is shown in Figure 5. Consider an electron originating from the source at S with direction SA. Because of the magnetic field normal to the plane of the diagram, its path is curved, with radius r, so that it reaches the detector at D. The angle $\delta$ is the difference between the true and measured ejection angles of the electron. The distance between the source and detector, SD, is 160 mm. It is clear from the diagram that the error in angle is given by

$$\delta = \arcsin\left(\frac{80}{r}\right)$$

and, for small angles

$$\delta \simeq \frac{80}{r} \times 57.3^\circ \quad .$$

The equation of motion of an electron in a magnetic field is

$$r = 3.37 \times 10^{-3} \frac{\sqrt{V}}{B} \text{ mm} \quad ,$$

where V is the electron energy in eV and B is the magnetic field strength in tesla. Therefore

$$\delta = \left(\frac{80 \times 57.3}{3.37 \times 10^{-3}} \frac{B}{\sqrt{V}}\right)^\circ$$

$$= 1.36 \times 10^4 \frac{B}{\sqrt{V}}^\circ \quad .$$

Figure 6a shows the value of $\delta$ for 1 and 5 eV electrons plotted against

the magnetic field strength in μT. If an average transverse field of 1 μT was present, the angular error for a 1 eV electron would be approximately 1.5°.

(b) Error in energy

The consideration of the trajectory of a charged particle in both electric and magnetic fields is, in general, very complicated. Therefore, to obtain an estimate of the error in energy induced by a magnetic field, the forces it will induce have been compared with the force due to the analysing electric field. To make this comparison it was assumed that the magnetic field is always perpendicular to the electron path. Therefore, for an electron of velocity v, the magnetic force is

$$F_B = Bev = Be\frac{\sqrt{2eV}}{m} \quad , \tag{4}$$

the electric force is

$$F_E = eE \tag{5}$$

and, from the design of the analyser,

$$\frac{4xE}{V} = 1 \quad . \tag{6}$$

The ratio of the two fields, from Equations 4-6, is

$$\frac{F_B}{F_E} = \frac{B}{\sqrt{V}} \; 4x\sqrt{\frac{2e}{m}}$$

$$= 3.6 \times 10^4 \; \frac{B}{\sqrt{V}}$$

where B is in tesla. In Figure 6b this ratio, interpreted as a measure of the error in the energy measurement, is shown for 1 and 5 eV electrons as a function of magnetic field strength. Again for a 1 eV electron and a 1 μT field, the error in energy would be 3.5 per cent.

To annul the earth's magnetic field, three pairs of octagonal coils were set up orthogonally. Octagonal coils were used since the formers could easily be made from light aluminium channel. The Helmholtz spacing for octagonal coils is 1.025 times the radius of the inscribed circle [Rankine 1934]. Values of 'maximum usable volume' for a given field uniformity have been published for circular and square coils [Cacak & Craig 1969]. As the results for these two types of coil are substantially the same, they may be assumed to apply also in the case of

octagonal coils. Cacak & Craig show that 1 per cent uniformity can be obtained throughout a volume of more than 0.16 $r^3$, where r is the coil radius. As the radii of the octagonal coils were made as large as was convenient (500 mm), the usable volume is $2 \times 10^7$ $mm^3$, or a sphere of radius 168 mm, adequate to contain the 160 mm electron paths.

As the earth's field at Sydney, New South Wales, is 40 μT, it should be possible to reduce the field so that it was never more than 0.4 μT. In practice, it was possible to reduce the field so that it was never more than 1 μT; the failure to achieve the theoretical value is probably due to field gradients caused by iron structures in the laboratory. Small perturbations were also caused by the welds in the stainless steel vacuum vessel.

## 4. APPARATUS TESTS

Initially there were difficulties due to very large background electron count rates. These spurious counts were partly removed by careful attention to the proton collimator and its alignment with the input slit of the analyser. The intensity of the remaining electrons, although still large, was proportional to the background gas pressure. These electrons seemed to owe their existence to the high reflectivity of slow electrons. Therefore, although the rate of electron production was not great, the background gas pressure being about $10^{-4}$ Pa, large numbers were built up because of the low absorption rate. This problem was solved by biasing the whole analyser assembly at -50 V, so that any electrons leaving the analyser region would be accelerated to the walls of the vacuum chamber and be most unlikely to return.

To gain an understanding of the behaviour of the apparatus, the following tests have been made:

(i) A small retarding potential difference (RPD) energy analyser was incorporated between the detector defining aperture and the channeltron. RPD scans were made for various values of analyser voltage, the electrons being produced by collisions between the proton beam and air as target gas. The scans were recorded directly by an XY recorder, the X axis being driven by the RPD voltage, the Y by a ratemeter driven by the channeltron output pulses. A typical example is shown in Figure 7. The true signal, formed by taking the difference of the two measured curves, is a typical RPD curve for a monoenergetic beam, namely a constant current falling fairly rapidly to zero at the beam energy.

The poor energy resolution can be attributed to the rough nature of the RPD analyser. As this analyser had to be small enough to fit between the detector slits and the channeltron, it was not easy to set up a configuration which would produce a uniform plane electric field.

(ii) A rough angular analysis of the electrons reaching the detector slit was made in the plane of the analyser plates. The detector aperture was replaced by two narrow slits perpendicular to the focal line. These slits were about 25 mm apart and a small pair of electrostatic deflection plates was placed between them. By varying the deflecting field, an angular analysis of the electrons was made perpendicular to the focal direction. The result of such a scan is shown in Figure 8. Again, because of the compact nature of the angular analyser, it is not possible to give a meaningful quantitative estimate of the cross section of the gas jet. It is quite clear, however, that the signal electrons originate from a localised region. The ratio of signal to background is better for angles near 90° and worse for angles near zero, as would be expected, because of the varying beam path length that can readily contribute to the background count rate.

(iii) A possible source of electrons could be the secondary electron emission from the analyser slits induced by protons elastically scattered onto the slits. Calculations show that the number of electrons formed in this way should not be significant; this was confirmed by two tests.

In the first test, the proton beam was deflected electrostatically to pass close to one or other of the edges of the slit. Gas was admitted to the jet assembly and an energy analysis was made of the electrons. The result was compared with one made with the beam centralised; no significant difference was noted. As the intensity of elastic scattering rises steeply with decreasing angle, the number of protons striking the slit edges would increase greatly when the beam was off centre. The fact that no increase in electron count rate was observed indicates that the effect is not an important one in the present experimental configuration.

In another test, the angular analysis described in Section 3 was carried out with the proton beam deflected electrostatically to such an extent that electrons were produced by collisions with the

slit edges. The angular distribution of these electrons can be seen, from Figure 9, to differ significantly from that obtained with electrons produced by the gas jet.

## 5. TRIAL MEASUREMENT

A preliminary measurement was made of the energy distribution of the electrons ejected at 30° by 50 keV protons incident on air. The raw data, in the form of an XY recorder trace, are shown in Figure 10. Measurements of the difference between the signal and background traces were made for a number of energies. These intensities were then divided by E to allow for the fact that the width of the energy window of the analyser is proportional to the energy, E. These corrected intensities were then normalised so that when plotted together with the results of Crooks & Rudd [1971], the differences and similarities between the two measurements would be most clearly demonstrated. As can be seen in Figure 11, the agreement between 30 and 100 eV is good but the present results below 30 eV do not show the same marked increase in intensity at low energies as was found by Crooks & Rudd.

These authors admit that the reproducibility of their measurements deteriorates below 12 eV electron energy and becomes completely unreliable below 3 or 4 eV. Furthermore, their cross section for 300 keV protons in nitrogen differential in energy alone (obtained by integration over all angles) is inconsistent with the results of Toburen [1971] for electron energies below 30 eV. At 13 eV, the cross section obtained by Crooks & Rudd [1971] is 1.6 times the Toburen result. It is therefore quite possible that the low energy results of Crooks & Rudd are too high by a factor of around 1.5.

To examine the other possibility, that the present results are in error, several factors have been considered as possible causes of a low measured count rate in the present experiment.

(a) A falloff in detector efficiency for low energy electrons
A test in which the potential of the cathode of the channeltron was varied over 100 volts with very little effect on the count rate indicates that this is not a major effect.

(b) Absorption of electrons by background gas Taking $10^{-15}$ $cm^2$ [Hasted 1972] as the total electron scattering cross section, it can be calculated that only about 1 per cent of the electrons are scattered over their 200 mm flight at a pressure of 2.67 mPa.

(c) Stray electric and magnetic fields The effects of stray fields was given by Crooks & Rudd as the probable reason for their difficulties with low energy electrons; the same difficulties could apply to the present apparatus. However, the field strengths that might be expected would not perturb 10 or 20 eV electron paths to any great extent.

Further data collection may resolve the lack of agreement at low electron energies. Fortunately, from the standpoint of radiation dosimetry, the precise direction and energy of low energy electrons is not of prime importance as, by their nature, these electrons will not travel far before absorption.

## 6. CONCLUSION

The feasibility of combining the principles of the 30° electrostatic energy analyser and the 'fountain' concept to make an apparatus capable of measuring angular and energy distributions of secondary electrons has been demonstrated. A variety of diagnostic experiments have been performed. A measurement at one angle, using air as the target gas, is in good agreement with published results at electron energies above 30 eV.

## 7. REFERENCES


Bewley, D.K. [1968] - *Radiat. Res.*, 34 : 446.

Cacak, R.K. & Craig, J.R. [1969] - *Rev. Sci. Instrum.*, 40 : 1468.

Crooks, G.B. & Rudd, M.E. [1970] - *Phys. Rev. Lett.*, 25 : 1599.

Crooks, G.B. & Rudd, M.E. [1971] - *Phys. Rev.*, 3 : 1628.

Green, T.S. & Proca, G.A. [1970] - *Rev. Sci. Instrum.*, 41 : 1409.

Harrower, G.A. [1955] - *Rev. Sci. Instrum.*, 26 : 850.

Hasted, J.B. [1972] - Physics of Atomic Collisions. Butterworths, p.309.

ICRU [1970] - Linear Energy Transfer. International Commission on Radiological Units and Measurements Report 16.

Kuyatt, C.E. & Jorgensen, T. [1963] - *Phys. Rev.*, 130 : 1444.

Rankine, A.O. [1934] - *Proc. Phys. Soc., (London)*, 46 : 14.

Rudd, M.E. & Jorgensen, T. [1963] - *Phys. Rev.*, 131 : 666.

Rudd, M.E. [1975] - *Radiat. Res.*, 64 : 153.

Rudd, M.E., Sautter, C.A. & Bailey, C.L. [1966] - *Phys. Rev.*, 151 : 20.

Rudd, M.E., Toburen, L.H. & Stolterfoht, N. [1976] - *At. Data Nucl. Data Tables*, 18 : 413.

Schmitz, W. & Mehlhorn, W. [1972] - *J. Phys. E. (London)*, 5 : 64.

Toburen, L.H. [1971] - *Phys. Rev.*, 3A : 216.

Toburen, L.H. & Wilson, W.E. [1972] - *Phys. Rev.*, 5A : 247.

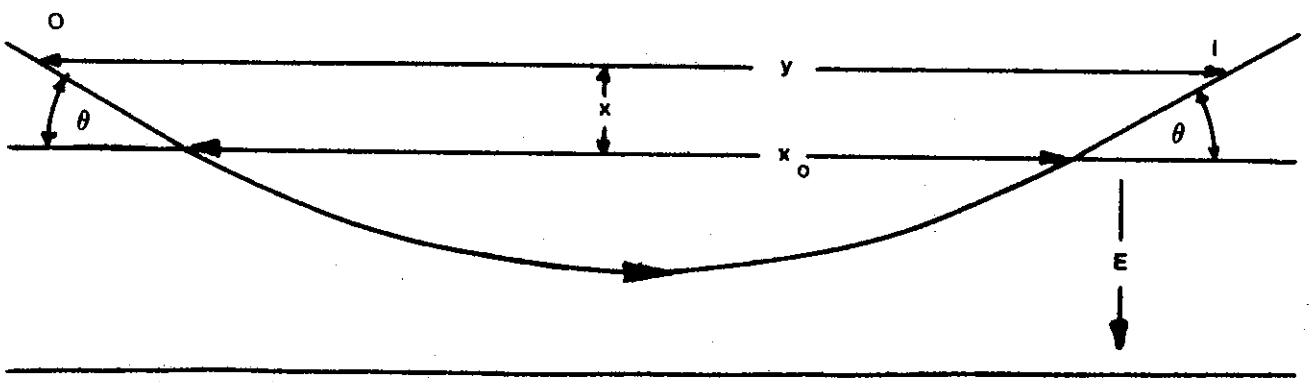


FIGURE 1. GEOMETRIC DIAGRAM FOR DERIVATION OF PRINCIPLES OF 30° ANALYSER

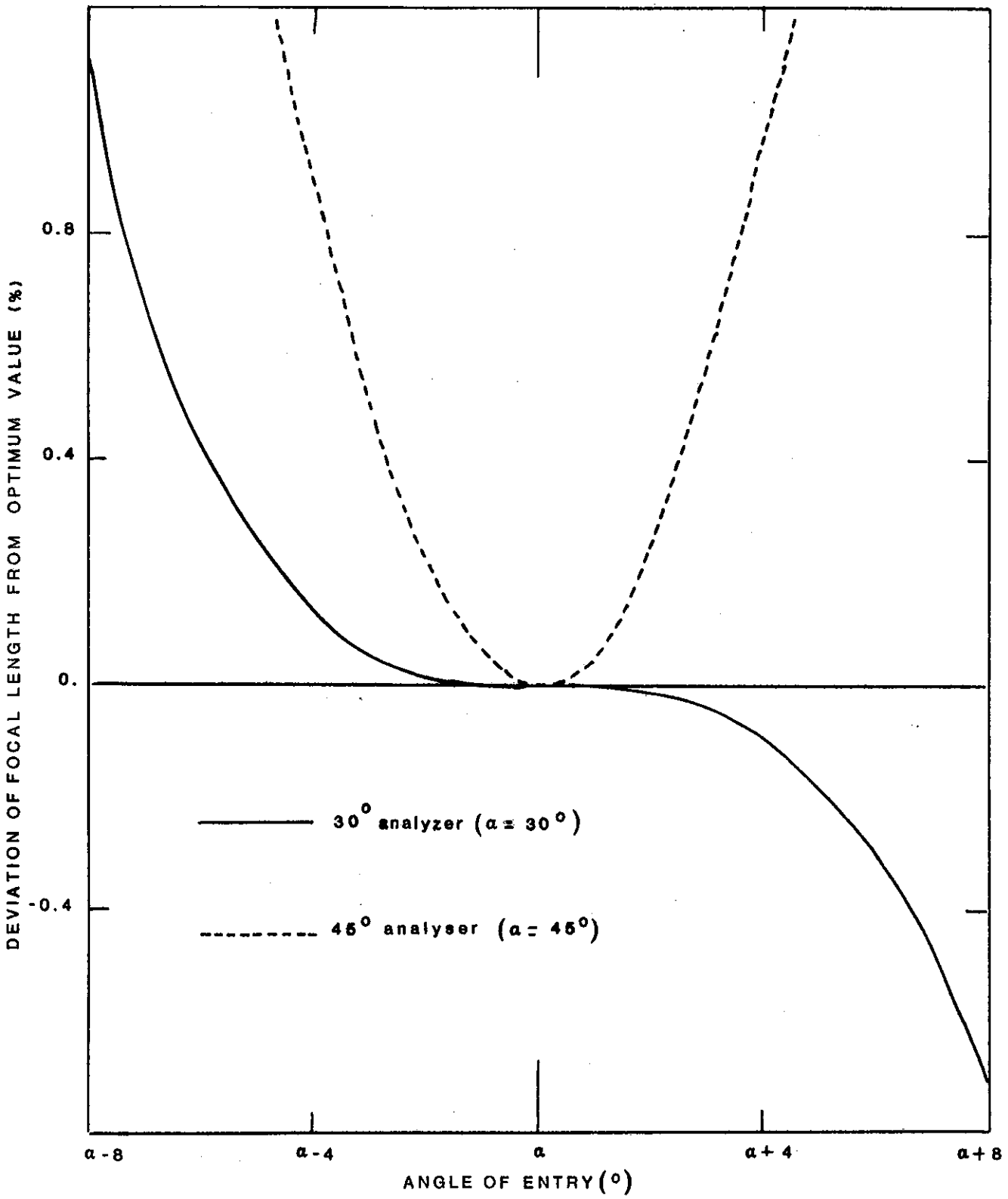


FIGURE 2. PERCENTAGE CHANGE IN FOCAL DISTANCES FOR 45° AND 30° ELECTROSTATIC ANALYSERS AS FUNCTION OF INPUT ANGLE

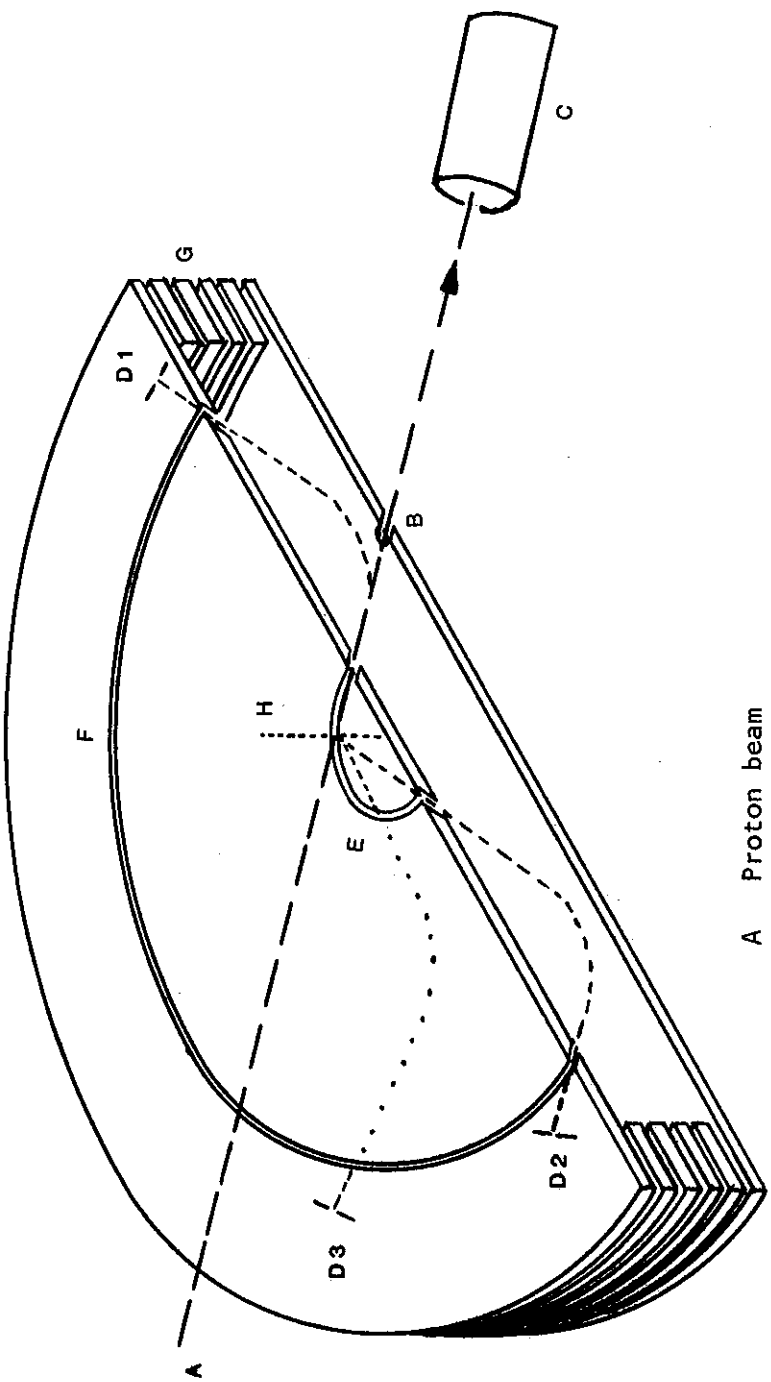


A Proton beam
B Beam exit hole
C Proton collector
D Electron detector apertures: 1, 0°; 2, 120°; 3, ~100°
E Entry slit
F Exit slit
G Guard rings
H Gas jet

FIGURE 3. CROSS-SECTIONAL SKETCH OF ELECTRON ENERGY ANALYSER

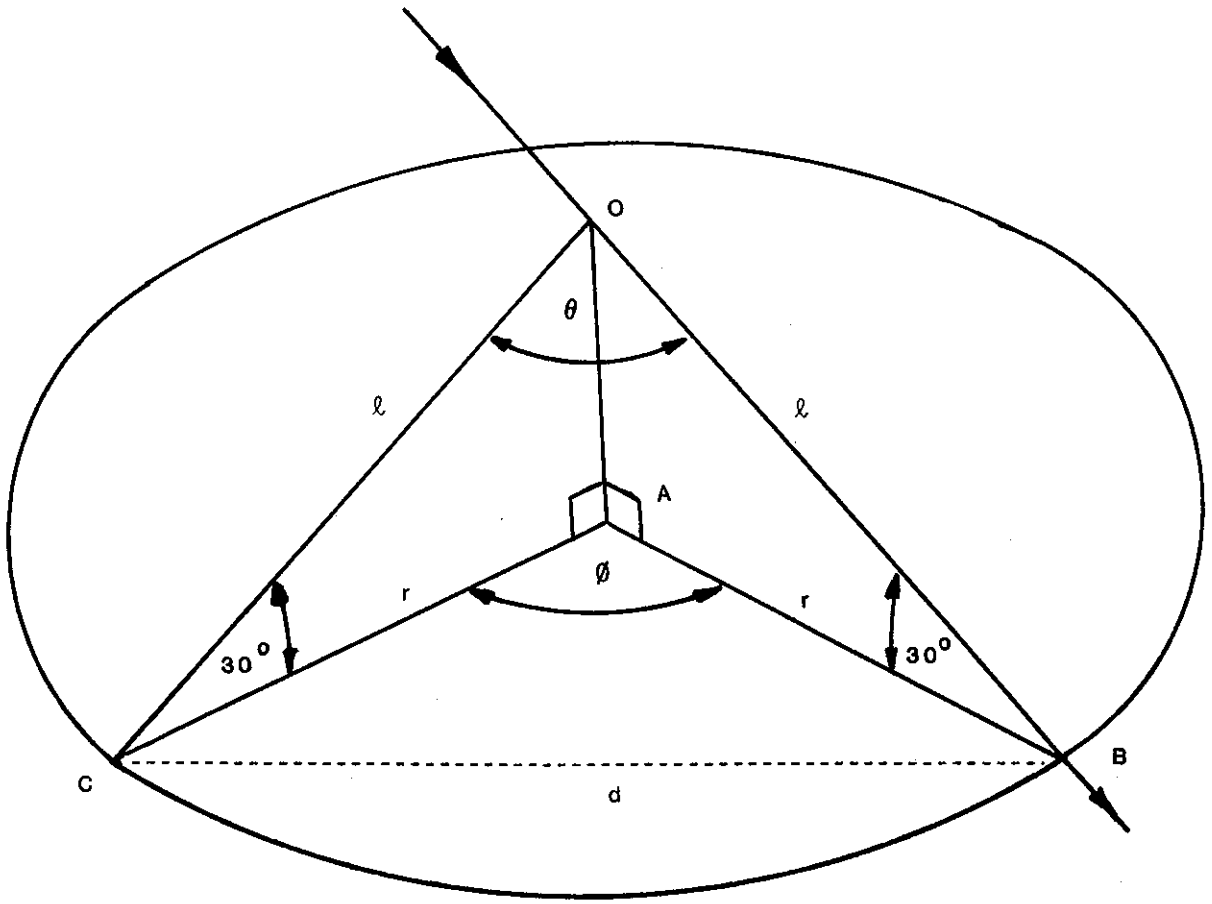


O = electron source

OB = proton beam

OC = electron ejected at angle θ

Points A, B and C lie on analyser input plane

B and C are two points on circular input slit

Ø is the angle on analyser plane that corresponds with the scattering angle θ

In Δ ABC $d^2 = 2r^2 - 2r^2 \cos \text{Ø}$

In Δ OBC $d^2 = 2\ell^2 - 2\ell^2 \cos \theta$

In Δ OAB $r = \ell \cos 30°$

These equations lead to

$$\cos \text{Ø} \; \frac{4 \cos \theta - 1}{3}$$

**FIGURE 4. RELATION BETWEEN $\theta$ AND $\phi$**

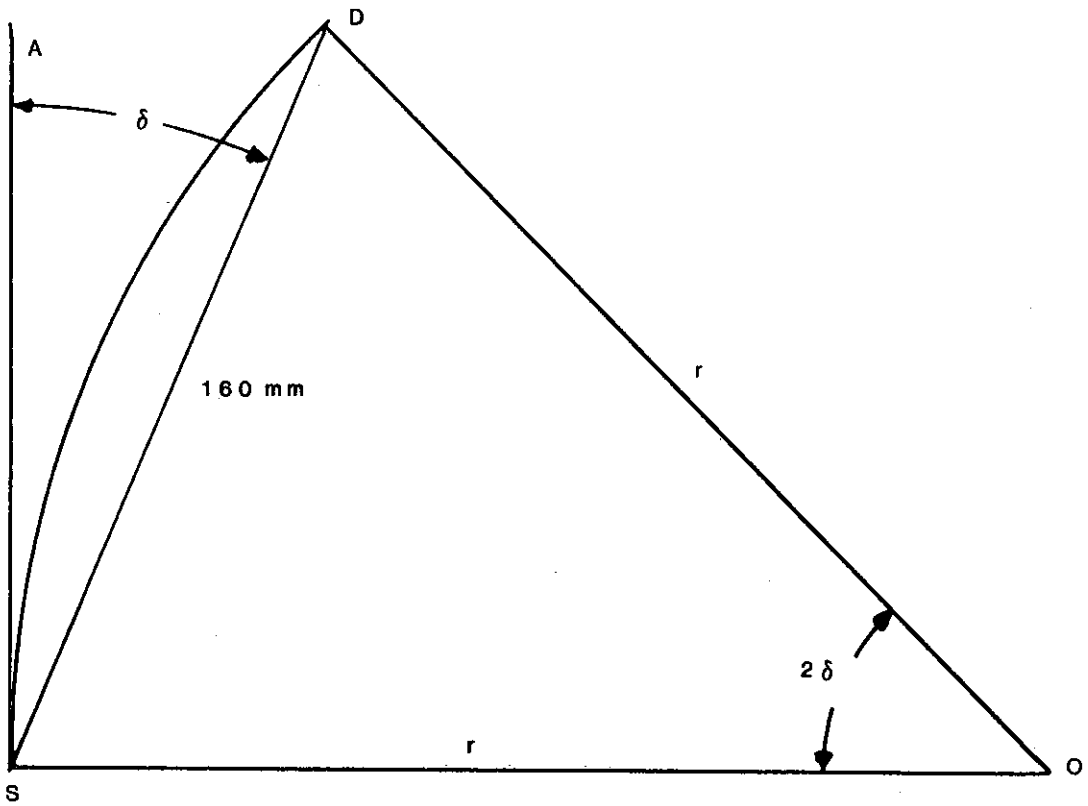


S Source of electrons
D Detector position
SA Direction of ejection of electron
SD Apparent direction of electron
r Radius of curvature due to magnetic field
δ Error in angle

**FIGURE 5. DIAGRAM FOR CALCULATION OF ERROR IN ANGLE MEASUREMENT DUE TO MAGNETIC FIELD**

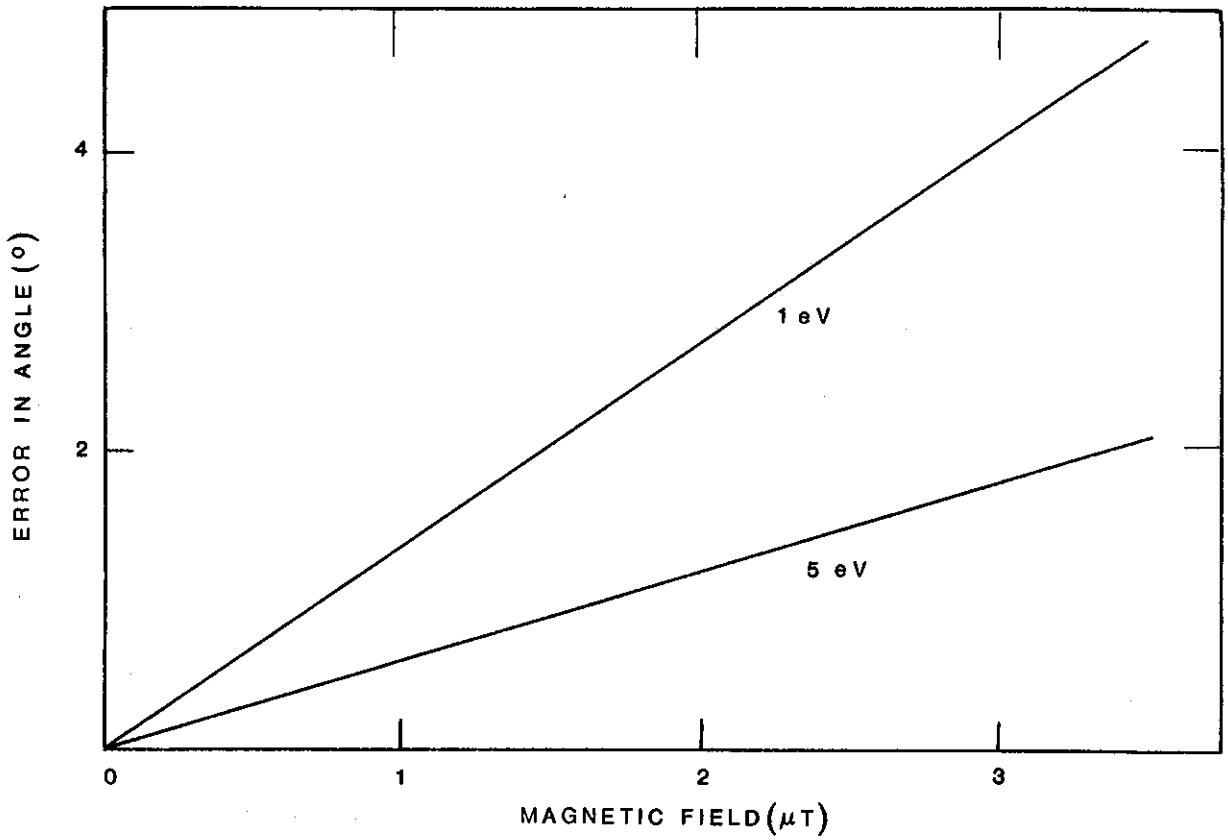


**FIGURE 6(a) ERROR IN MEASURED SCATTERING ANGLE AS FUNCTION OF MAGNETIC FIELD**

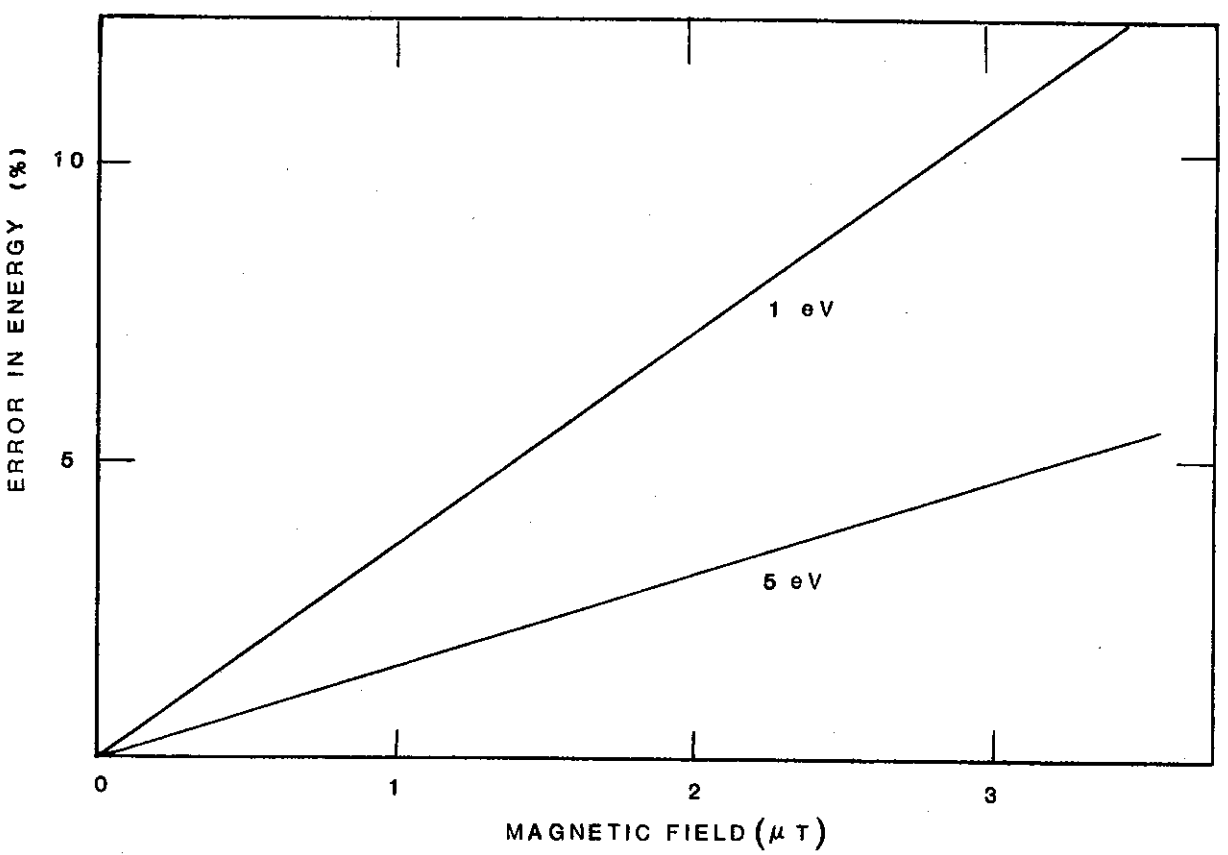


**FIGURE 6(b) ERROR IN MEASURED ENERGY AS FUNCTION OF MAGNETIC FIELD**

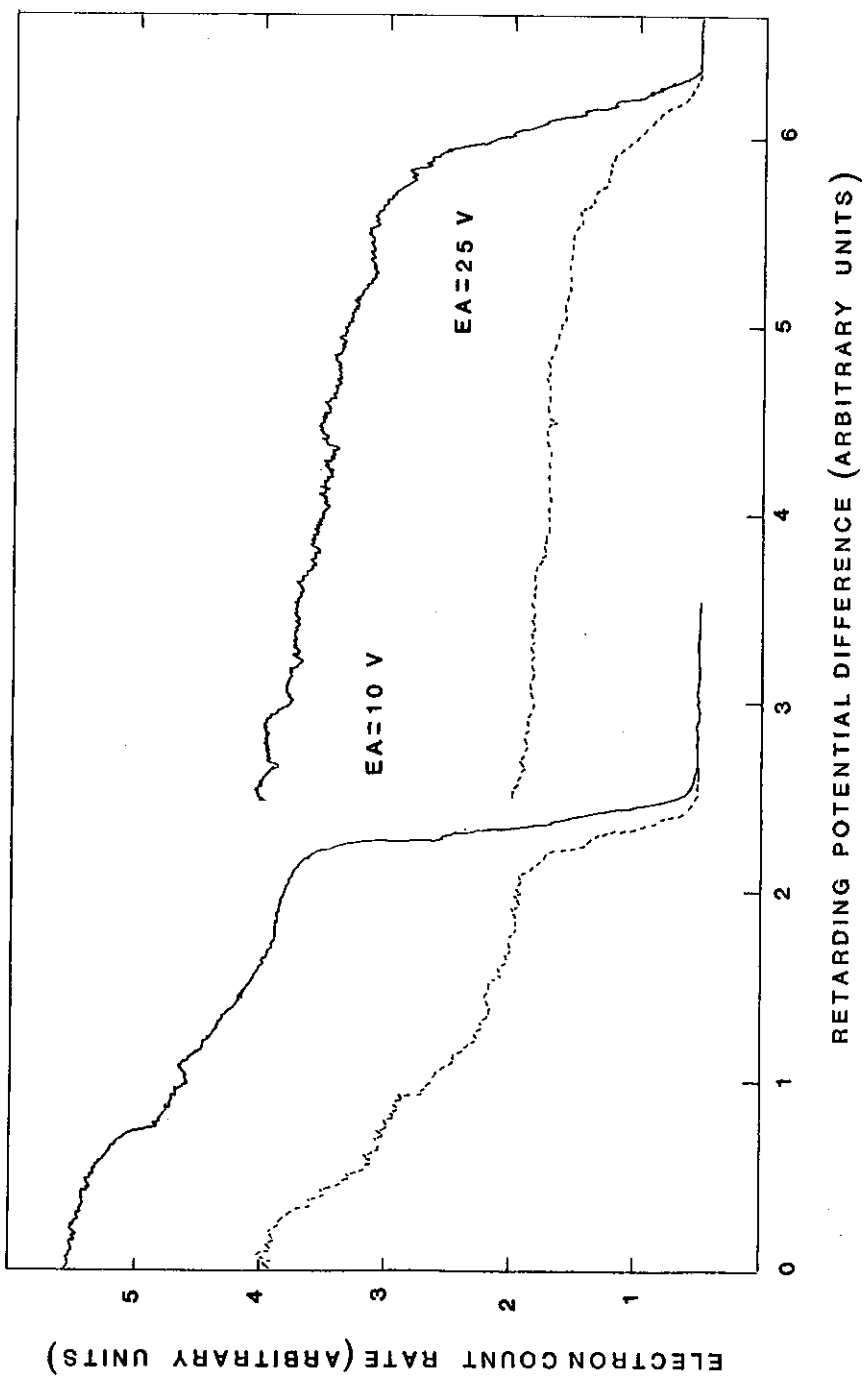


FIGURE 7. RETARDING POTENTIAL DIFFERENCE CURVES FOR ELECTRONS EMERGING FROM ANALYSER AT TWO DIFFERENT ANALYSER VOLTAGES. (Curves are presented for air admitted through the jet (solid) and for air admitted through a leak valve to bring the background gas to the same value (2.7 mPa) in both cases (dotted))

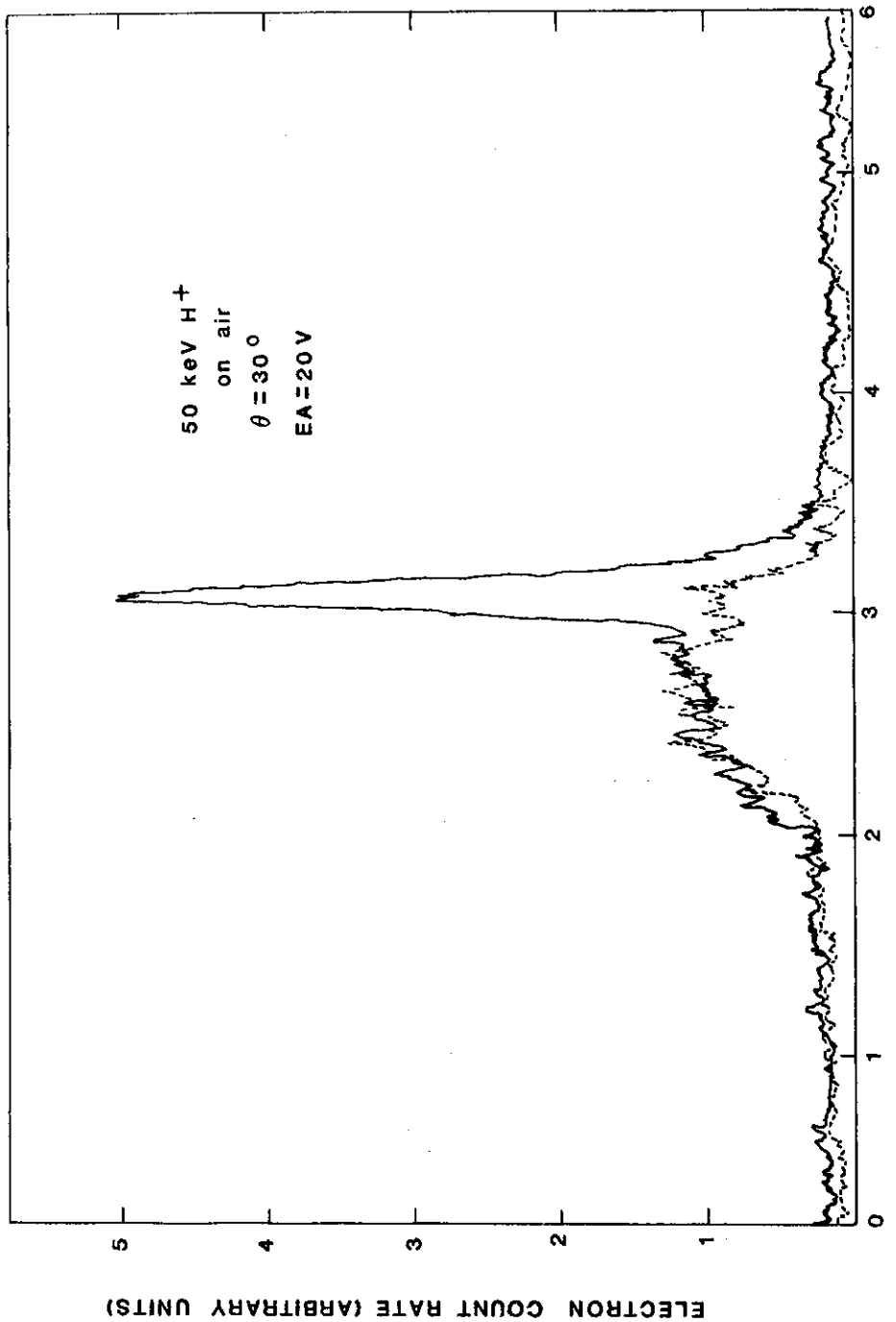


FIGURE 8. ANGULAR ANALYSIS OF ELECTRONS ENTERING DETECTOR AT 30° POSITION WITH 20 VOLT ANALYSING POTENTIAL. (Curves taken with air admitted through jet (solid) and with background adjusted to be equal to that produced by the jet (dotted). Most of the background electrons originate along the beam after it has passed through the jet and has entered the analyser. The beam before the jet is largely shielded by the collimating tube. The asymmetry of the background curve, with respect to the signal peak, is due to this effect.)

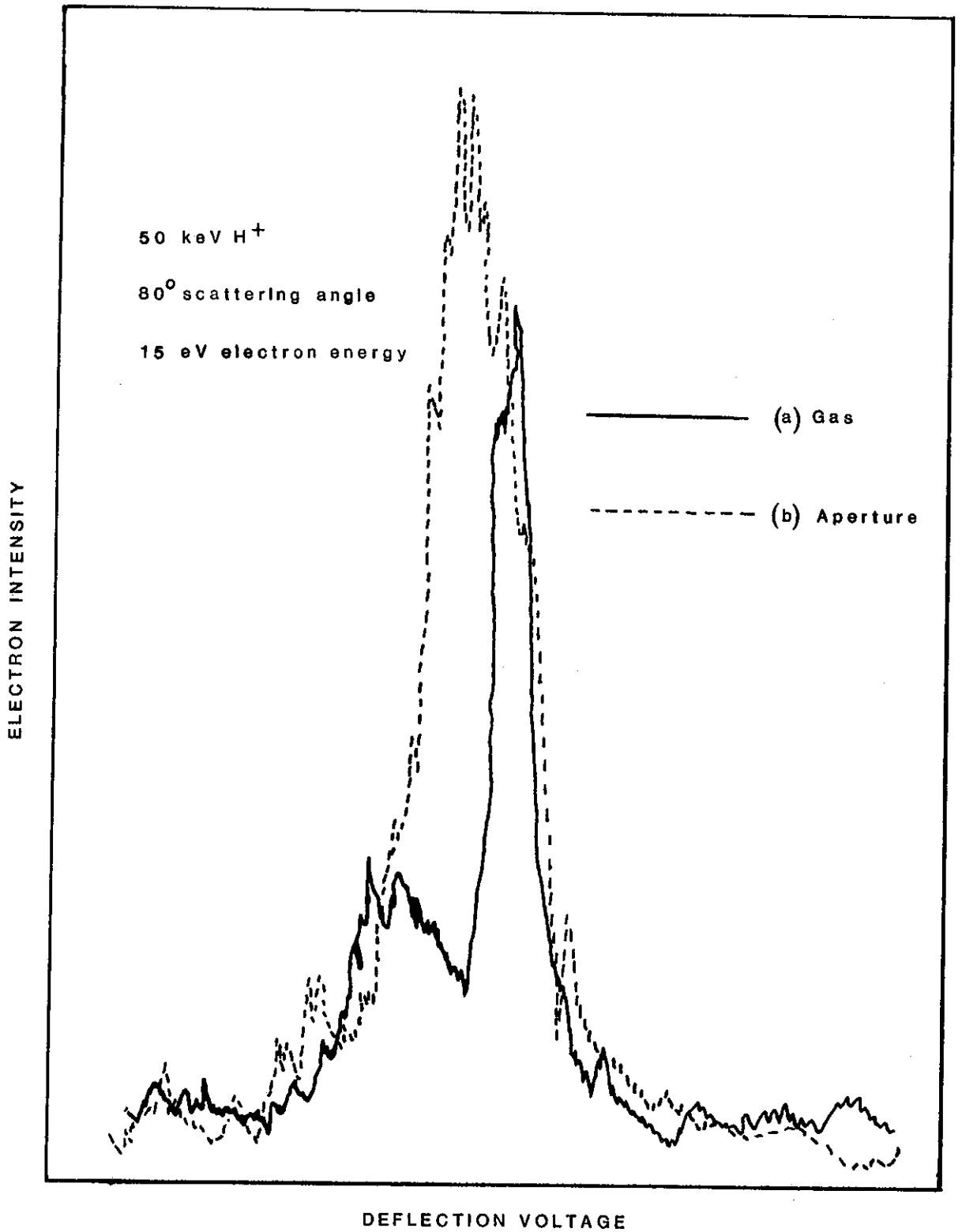


FIGURE 9. RECORDINGS OF ANGULAR DISTRIBUTIONS OF ELECTRONS PRODUCED AS A RESULT OF (a) ADMITTING AIR THROUGH JET (b) DEFLECTING PROTON BEAM TO CAUSE SOME PROTONS TO STRIKE THE APERTURE EDGE

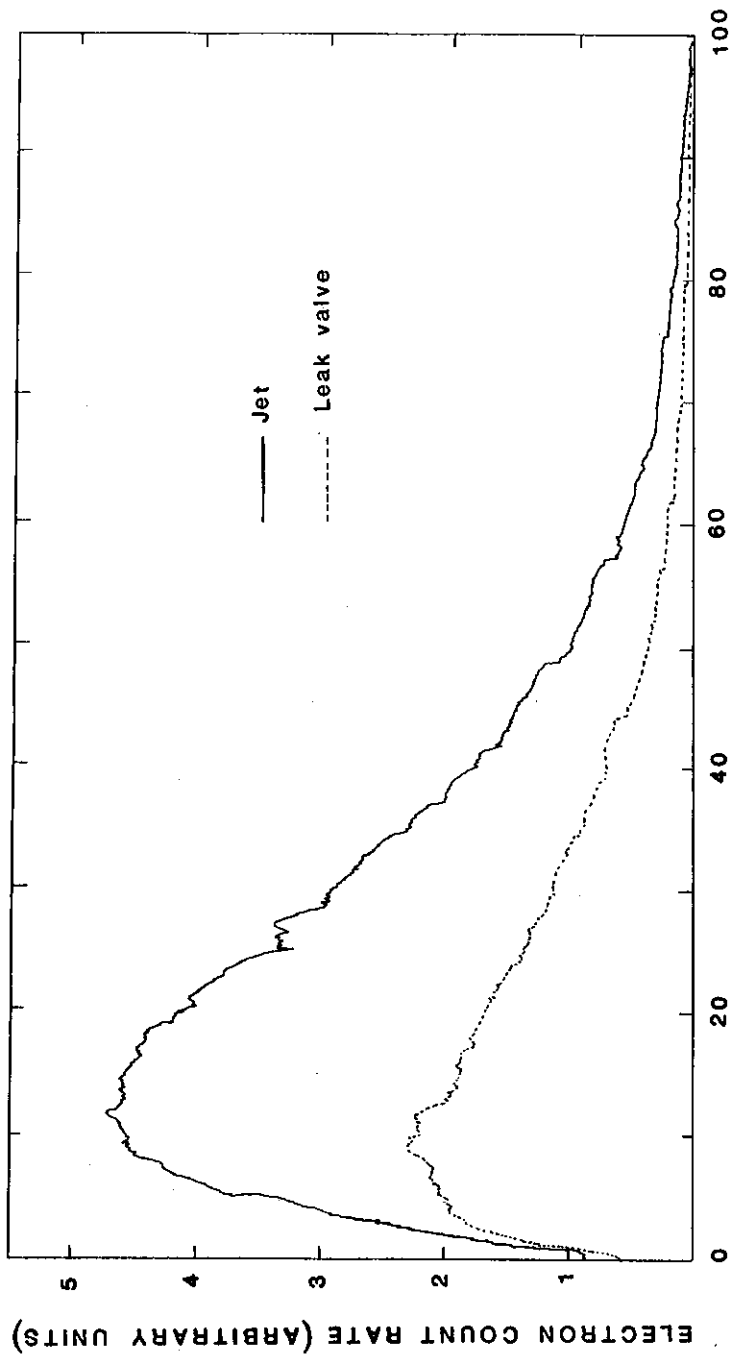


FIGURE 10. BASIC ENERGY ANALYSIS CURVE FOR ELECTRONS EJECTED AT 30° BY 50 keV PROTONS ON AIR. (The background gas pressure has been adjusted by means of a leak valve to be equal for the two measurements.)

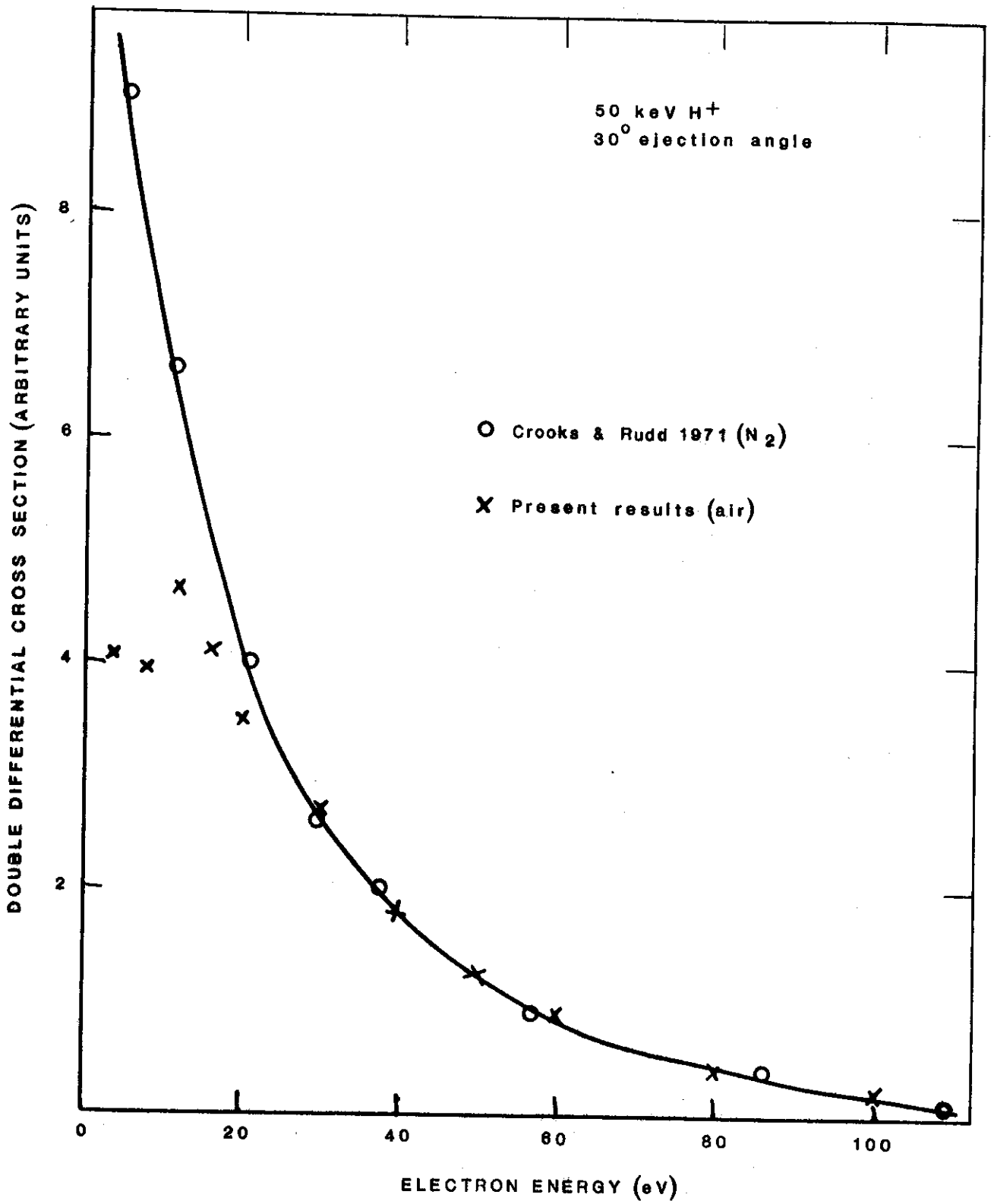


FIGURE 11. PRELIMINARY MEASUREMENT OF ELECTRON ENERGY DISTRIBUTION USING AIR AS TARGET GAS COMPARED WITH PUBLISHED RESULTS FOR $N_2$